Climatological relationships among the moisture budget components and rainfall amounts over the Mediterranean based on a super-high-resolution climate model

Fengjun Jin,[1] Akio Kitoh,[2] and Pinhas Alpert[1]

Received 15 February 2010; revised 20 December 2010; accepted 18 February 2011; published 7 May 2011.

[1] Moisture budget components over a rectangular region defined by the longitudes 6.0°W–36.0°E and latitudes 30.0°N to 45.0°N, with an area of about 6.08×10^6 km^2 over the Mediterranean (Med) Basin, are studied by the use of the Japan Meteorological Agency super-high-resolution (20 km) GCM monthly mean data. The research time periods are 1979–2007 for current run and 2075–2099 for future run. Six rainy months of October to March with a total of 168 months for the current run and 144 months for the future run were selected. The rain months have been categorized into five groups of months based on the mean monthly rainfall amounts where the five groups are $P < 1.0$, $1.0 \le P < 1.5$, $1.5 \le P < 2.0$, $2.0 \le P < 2.5$, and 2.5 mm/d $\le P$. We found that generally, over the Mediterranean, the outflow-inflow is balancing the independently calculated evaporation-precipitation quite well with a correlation coefficient of about 0.89. The present seasonal (October-March) precipitation simulated from the 20 km GCM showed a quite reasonable agreement with the CRU. The seasonal area mean precipitation and evaporation are 1.85 mm/d and 2.44 mm/d, respectively. The largest two precipitation categories contribute over 50% of the total seasonal rainfall. The evaporation varies positively with the precipitation for all precipitation categories. Also, the relatively high mean recycling ratio (55%) indicates that the local Med evaporation has a central role in the local precipitation. Another important finding is that the decreasing trend of recycling ratio with the rising of the precipitation category implies that the outside moisture inflow role increases with the increase of the precipitation category. For all the precipitation categories, the total outflow is larger than the total inflow, indicating that the Med area is an important source of moisture. Individual boundary moisture flux shows that the main moisture comes from the west boundary and contributes 59% of the total inflow, while the main outflow is through east boundary and is responsible for 46% of total outflow. Analysis of monthly precipitation indicates that the October and November have the two largest amount of precipitation over the research region. The moisture budget study separated for the east and the west Med shows that the area mean precipitation for the east and the west Med are 2.14 and 2.29 mm/d, while the evaporation are 4.48 and 3.59 mm/d. The plausible reason for the differences between these two basins has been discussed. The moisture supplies to the east Med is mainly from the west boundary, while for the west Mediterranean, the north boundary inflow also plays an important role along with the west boundary. The future moisture budget components over Med suggest that the precipitation is decreasing from 1.85 to 1.62 mm/d and the evaporation is increasing from 2.44 to 2.56 mm/d between current and future. Another finding is that the largest precipitation number of months decreases from 12% to only 6% of the total number of months, while the intensity of the precipitation in this category enhances in the future.

Citation: Jin, F., A. Kitoh, and P. Alpert (2011), Climatological relationships among the moisture budget components and rainfall amounts over the Mediterranean based on a super-high-resolution climate model, *J. Geophys. Res.*, *116*, D09102, doi:10.1029/2010JD014021.

[1]Department of Geophysics and Planetary Sciences, Tel-Aviv University, Tel-Aviv, Israel.
[2]Meteorological Research Institute, Tsukuba, Japan.

0148-0227/11/2010JD014021

1. Introduction

[2] The Mediterranean (Med) as a transition zone between humid climates to the north and arid climates to the south plays a unique role in the influence of climate on its sur-

rounding areas. Lack of water is a specific feature over this densely populated region, particularly over the Middle East and south region. The water shortage may become even worse under global warming and make this region extremely vulnerable to any (natural or anthropogenic) reductions in available surface water, rendering it highly sensitive to changes in climate. The sharper warming trends due to global warming makes the topic of water resources much more crucial [*Ziv et al.*, 2005] over the Med region, as also reported by the Intergovernmental Panel on Climate Change (IPCC) Fourth Assessment Report (AR4) [*Intergovernmental Panel on Climate Change* (*IPCC*), 2007]. Therefore the better understanding of the features of the atmospheric moisture budget components (MBC), especially the relationships between other MBC and the rainfall amount, as well as its change in the future over this region, is of great significance. This topic is also of great importance for all Mediterranean countries for future decision making which is related to the climate change.

[3] The exact mechanism controlling precipitation in the Med region is complex, and precipitation amounts and their distributions are largely affected by the topography and land-sea distribution [*Ozsoy*, 1981]. Moreover, earlier studies have shown that the precipitation regime of the Med region has significant teleconnections. *Hurrell and van Loon* [1997] studied the relation between the climate change and the North Atlantic Oscillation (NAO); *Mariotti et al.* [2002b] showed that the precipitation of the Med region has strong correlation with NAO. Other teleconnections also have close relation with the precipitation of the Med, such as El Niño Southern Oscillation (ENSO) [*Fraedrich and Mueller*, 1992; *Fraedrich*, 1994; *Price et al.*, 1998; *Diaz et al.*, 2001; *Mariotti et al.*, 2002a] and variabilities of South Asian Monsoon and Africa Monsoon [*Reddaway and Bigg*, 1996; *Rodwell and Hoskins*, 1996; *Ziv et al.*, 2004], as well as the large increase in Red Sea trough frequencies [*Alpert et al.*, 2004] and also teleconnection to tropics and tropical cyclones [*Alpert et al.*, 2005; *Krichak et al.*, 2004].

[4] Since the linkages between atmospheric dynamics, water vapor conditions, and precipitation are constrained by the moisture budget equation, moisture budget analysis is an attractive tool for studying the processes that generate precipitation [*Zangvil et al.*, 2001]. During recent decades, a wide range of moisture budget studies has been published. Some of the studies focused on the annual climatology of water vapor for global or hemispheric scales [*Starr and Peixoto*, 1958; *Starr et al.*, 1965], while others concentrated on the hydrology of large regions [e.g., *Rasmusson*, 1967, 1968; *Peixoto*, 1973; *Mariotti et al.*, 2002a, 2002b, 2008; *Jin et al.*, 2010].

[5] Little research has been done on the moisture field in the Med region before the appearance of reanalysis data because of lack of sufficient surface and upper air data over this area. However, some studies have been carried out since the reanalysis data became available. *Alpert and Shay-El* [1994] studied the moisture source for the precipitation of the East Med; *Mariotti et al.* [2002a, 2002b] completed a detailed study on the hydrological cycle and water budget over the Med region; *Jin and Zangvil* [2010] investigated the relationships between moisture budgets components over the eastern Med.

[6] The climate model is an essential tool in order to study potential future climate changes. Recently, several studies investigated the climate changes over the Med region based on different climate models [*Gibelin and Deque*, 2003; *Alpert et al.*, 2008; *Giorgi and Lionello*, 2008; *Mariotti et al.*, 2008]. However, the global climate models (GCMs) have usually coarse spatial resolution of about 100–300 km; therefore they cannot capture well the small-scale factors which have important influence on the moisture budget field, especially over the complicated topographic region of the Med. On the other hand, the regional climate model (RCM) indeed has relative fine spatial and temporal resolutions compared to the GCM. But, besides RCMs are computationally expensive, they also need lateral boundary condition data, which come from the GCM in order to drive the RCM and strongly influence the final result. Most recently, a super-high-resolution 20 km grid GCM, which was developed at the Meteorological Research Institute (MRI) of the Japan Meteorological Agency (JMA), became available. The model can overcome the aforementioned disadvantages which exist in both the GCM and RCM. It avoids the problems of the unfit-in-scale of the lateral boundary condition but also can incorporate interactions between global scale and regional scale explicitly. The present study attempts to examine the moisture fields over the Med by using this super-high-resolution GCM, mainly focus on the relationships between the MBC and the rainfall amount, as well as the potential future changes in the MBC.

2. Data and Methodology

2.1. Data

[7] The super-high-resolution 20 km grids GCM is a climate model version of the operational numerical weather prediction model used in the JMA. A detailed description of the model is given by *Mizuta et al.* [2006].

[8] The monthly mean based parameters are contained in this data set. The two runs of the 20 km GCM cover the time periods 1979–2007 for current/control and 2075–2099 for the future. The control run used the observed monthly sea surface temperatures (SST) and sea-ice distribution, while the future run used the SST and sea-ice concentration anomalies of the multimodel ensemble projected by Coupled Model Intercomparison Project Phase 3 (CMIP3) under the Special Report on Emission Scenario (SRES) A1B emission scenario. Details of the method are found in the work of *Mizuta et al.* [2008].

[9] The global time series data set based on rain gauge measurements (land only) from the climate research unit (CRU) [*Mitchell and Jones*, 2005] was used here; it is also a monthly based data set. The grid horizontal resolution of the CRU is 0.5 × 0.5 degree, and the available time period is 1901–2002. We also used the Climate Prediction Center Merged Analysis of Precipitation (CMAP) compiled by *Xie and Arkin* [1997] and the Global Precipitation Climatology Project (GPCP) compiled by *Adler et al.* [2003].

2.2. Research Area and Study Time Period

[10] The full Med research area is located between 30.0°N to 45.0°N and 6.0°W to 36.0°E (Figure 1) with a total area of about 6 million km^2 or 6.08 × 10^6 km^2. In order to cover the entire Med basin, two other water bodies, which are part

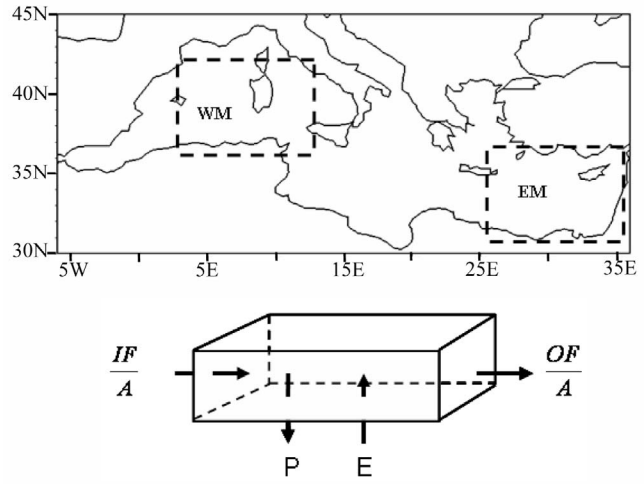

Figure 1. Research area (entire Mediterranean, the east and west Mediterranean) and schematic presentation of water vapor budget. For more details, see text.

of the Black Sea and Bay of Biscay, are also included in the research region as constrained by the method applied in this research, though these two water bodies will have a definite influence to the local evaporation and boundary moisture inflow or outflow. However, the areas of these two water bodies are relatively small compared with the Med area. Therefore it will not have a significant influence on the result due to these extra water bodies. In addition, two independent rectangular-shaped subbasins, which cover the eastern and western parts of the Med, respectively, were selected to study the specific feature of the MBC for these two different regions (Figure 1). The eastern part covers the area by longitude of 26–36°E and latitude of 31–37°N, while the western part by longitude of 3–13°E and latitude of 36–42°N, respectively. The area of each the two subbasins is of about 6.0×10^5 km^2; the east one is a bit larger than the west one. Also, to have an objective comparison, the two selected basins are almost covered by the same proportion of water body (about 90%).

[11] The current study period is 1979–2007 while 2075–2099 is for the future following the period of simulation of the 20 km GCM. Since this research will focus primarily on the relationships of other MBC with the rainfall amount, only the main rainy season, i.e., October-March, was investigated here. However, for the study the moisture flux seasonal features, the summer, i.e., June-August, is also included.

2.3. Water Vapor Budget Equations and Recycling Ratio

[12] Following *Rasmusson* [1968, 1971] and *Yanai et al.* [1973], and by ignoring the cloud liquid water advection, the traditional equation of the water vapor budget (WVB) per unit mass of air, can be written as:

$$\frac{\partial q}{\partial t} + \vec{V} \bullet \nabla q + \omega \frac{\partial q}{\partial p} = e - c \tag{1}$$

where q is the specific humidity, p is atmospheric pressure, $\vec{V}$ is the horizontal wind vector, ω is the vertical pressure velocity, and e and c are the cloud evaporation and condensation rates per unit mass. It should be noticed here, though, the cloud liquid water is less important in the balancing of the atmospheric water vapor budget. However, its potential importance in some regions has been discussed by *Shay-El et al.* [2000]. By using the mass continuity equation and vertical integration of equation (1), the traditional atmospheric moisture budget equation takes the form:

$$\frac{1}{g}\frac{\partial}{\partial t}\int_S^T qdp + \frac{1}{g}\int_S^T \vec{V} \bullet \nabla q dp + \frac{1}{g}\int_S^T q\nabla \bullet \vec{V} dp = E - P \tag{2}$$

where g is the acceleration of gravity, S and T indicate the Earth surface and top integration limits, respectively, and E and P are the surface evaporation and precipitation rates. The first term on the left side of equation (2) is the time change of atmospheric precipitable water (*dPW*), often called also "the storage term"; the second and third terms are the horizontal water vapor advection and the horizontal velocity divergence in the presence of moisture, respectively. The sum of the second and the third terms is the moisture flux divergence (MFD) that will be analyzed later. Using Green's Theorem, MFD can be expressed as [e.g., *Zangvil et al.*, 2004]

$$MFD = \frac{1}{g}\int_S^T \nabla \bullet q\vec{V} dp = \frac{1}{Ag}\int_S^T \int qv_n dl\, dp = \frac{OF}{A} - \frac{IF}{A} \tag{3}$$

where A is the area of the integrating region, v_n is the wind component normal to the region's boundary, dl is a length increment along that boundary, and *OF/A* and *IF/A* are the total water vapor outflow from and inflow into the region normalized to a unit area. Substitution of equation (3) into equation (2), and by ignoring the strorage term *dPW* as this term is relatively small for a climate research, yields

$$E - P = \frac{OF}{A} - \frac{IF}{A} \tag{4}$$

The advantage of equation (4) is that it clearly identifies the externally advected water vapor, IF/A, whereas MFD in equation (3) describes a mixture of processes within the region and on its boundaries and thus cannot be directly associated with a specific water vapor source.

[13] In order to quantify the relative contribution of water vapor originating from the local evaporation E versus the moisture originating outside the region, IF/A. We used the Recycling Ratio(R) formula introduced by *Zangvil et al.* [1992]:

$$R = \frac{E}{E + \frac{IF}{A}} \tag{5}$$

The physical meaning of R is that it refers to the process by which a portion of the precipitated water that has evapotranspired from a given area contributes to the precipitation P over the same area.

3. Results and Discussions

3.1. Verification of WVB Equation

[14] Without specific indication, the following discussions are related to the current run (1979–2007) of 20 km GCM.

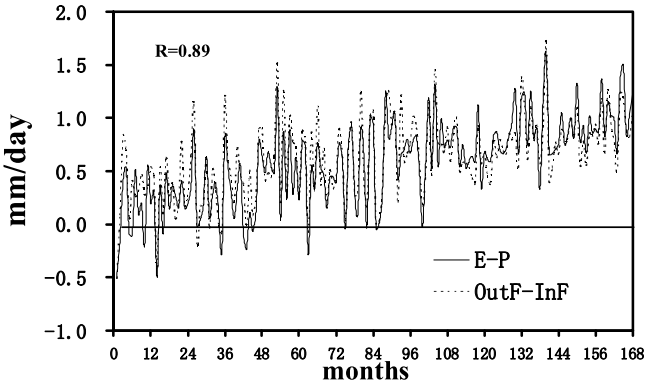

Figure 2. Variation of monthly area mean outflow-inflow and evaporation-precipitation sorted by the descending of precipitation for the rainy seasons (October to March) from 1979 to 2007. Hence month 1 is the month which got the highest mean precipitation while month 168 got the lowest. Unit are millimeters per day.

The MBC of E and P are directly derived from the 20 km GCM data, while the terms IF/A and OF/A are calculated from the water vapor flux data. In many moisture budget studies, the moisture budget equation is used to derive the unknown term of the MBC, such as E, as residuals [e.g., *Shay-El et al.*, 1999; *Zangvil et al.*, 2001]. Obviously, when such a procedure is carried out, the moisture budget equation is exactly balanced. However, in reality, it is difficult to obtain this balance, since errors inevitably exist in the process of data assimilation. Therefore it is necessary to examine how the separately calculated MBC terms in balancing the WVB equation (4).

[15] As shown in Figure 2, the long-term winter monthly mean moisture budget calculations over the Med show a quite reasonable balance between E-P and OF/A-IF/A with a correlation coefficient of 0.89, which is also statistical significant at 99% level. This value is higher than that of *Jin and Zangvil* [2010], in which study they got only 0.79 by using NASA reanalysis data. The mean value of difference between E-P and OF/A-IF/A is only about 0.15 mm/d. A close examination of Figure 2 will show that, compared to the E-P, the 20 km GCM somewhat overestimates/underestimates OF/A-IF/A for those months with large/small amount of P. It is not easy to give a definite explanation to this imbalance. Separate studies for the eastern and western Med show that the correlation coefficient between these two terms is even higher reaching 0.98 and 0.94, respectively. These results show the credibility of the present 20 km GCM data set for studying the balance of the WVB equation.

3.2. Examination of P and the Large-Scale Moisture Flux Fields

[16] Before going to the detailed discussions of the relationships among the MBC, it is essential to check how the MBC generated from the 20 km GCM fit with those which are based primarily on the observation data. Among all the components, the precipitation field is perhaps more attractive, though there are still great difficulties and uncertainties remaining regarding the precipitation estimates, especially over oceanic regions. This is not only because the precipitation data is relatively easy to obtain from the observation station (as compared to other components, such as E, or the vertically integrated horizontal moisture fluxes *qu* or *qv*) but also because its crucial role in the water cycle balance and the climate change over this sensitive region.

[17] Figure 3 shows that the wet season mean P from the 20 km GCM is quite consistent with the observed CRU P. Over the Med region, the latitudinal gradient is the predominant feature, with a drier area located to the south of the African coastline, and a wetter area over the northern coastline of the Med basin. However, a closer examination shows that the amount of the peak P generated in the 20 km model is somewhat larger than that of the CRU. For instance, this can be noticed over the Fertile Crescent, the south coast line of Black Sea, as well as in the Alpine mountain region. Does the larger P from 20 km GCM represent the reality of precipitation regime over the study area? *Jin et al.* [2011] showed that the 20 km GCM simulates very well the peak P over the Middle East region as compared with the CRU data. This was suggested to be largely due to the super-high spatial resolution GCM which is more sensitive in capturing the precipitation strongly influenced by the complex physiography. However, it is very important to emphasize here that the better performance of 20 km GCM in quantitatively simulation of the P does not conceal the fact that it does not describe the interannual change of P over the study area as good as compared to the other data sets, which are strongly based on observations. For instance, the CRU data is very good in generating of the Euro-Mediterranean winter rainfall and particularly the interannual variability [i.e., *Mariotti et al.*, 2002a]. Figure 4 shows

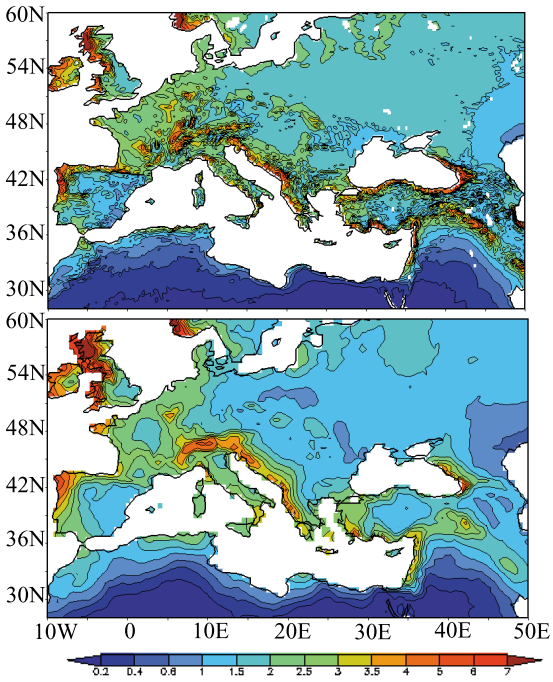

Figure 3. Long-term (1979–2002) mean precipitation of rainy season (October to March) from 20 km (top) GCM and (bottom) CRU. Unit are millimeters per day.

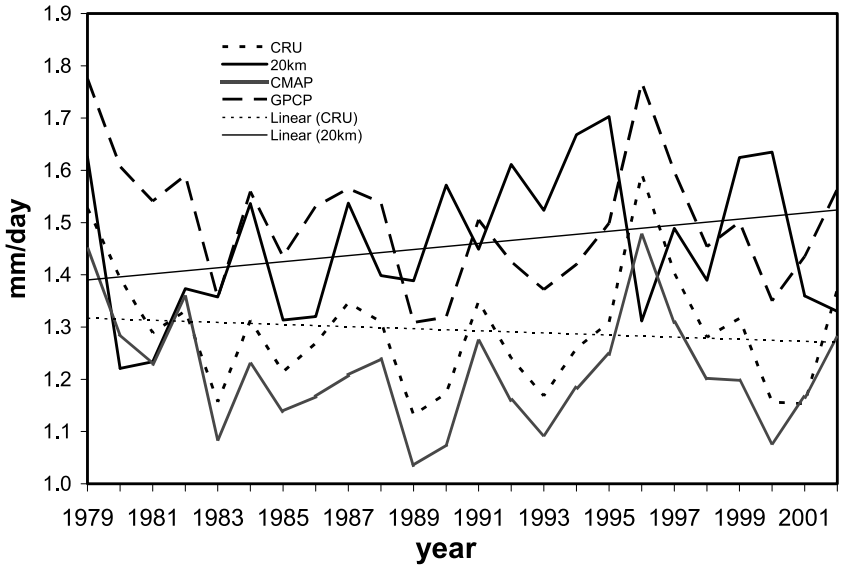

Figure 4. Long-term (1979–2002) interannual change of area mean precipitation over the Mediterranean (6°W–36°E, 30°N–45°N). The 20 km GCM and the CRU cover only the land area; the climate prediction center's merged analysis of precipitation (CMAP) and global precipitation climatology project (GPCP) cover both the land area and water body. The trend line for the change of precipitation are added only for the 20 km GCM and the CRU.

the interannual change of the area mean P over the land area of the Mediterranean from 1979 to 2002 for the 20 km GCM and the CRU and also for the land area and water body for the CMAP and GPCP. The long-term annual area mean P for these four data sets are quite close, with the values of 1.46, 1.29, 1.22, and 1.5 mm/d, for the 20 km, the CRU, the CMAP, and the GPCP, respectively. The similar pattern is found for the interannual change of P for the CRU, CMAP, and GPCP, though the CMAP and GPCP are with a coarser resolution, i.e., 2.5 degree by latitude and longitude, but with some small difference in the magnitude. However, the P trend shows opposite signs for the 20 km GCM and the rest of the three data sets. It is slightly increasing in the 20 km GCM, but decreasing for the other three data sets; *Alpert et al.* [2002] discussed this observed decreasing trend by using rain gauge data. These results indicates that the 20 km GCM data has poor performance in simulating the interannual change of P as compared to the other three data sets which are based on the observation data. Therefore cautions should be paid if climate model data is used in performing interannual related research.

[18] It is also interesting to note that, except for the mean P in Figure 4 which are very close among these four data sets, the P interannual standard deviations (SD) in the four data sets are not very different, MRI-AGCM-20 km (0.14), CRU (0.12), CMAP (0.11), and GPCP (0.12). As is well known what we should really expect from a good climate model are similar means and SDs, not necessarily the interannual changes.

[19] The moisture flux fields are also investigated to study how the 20 km GCM data is in describing these fields. Figures 5a and 5c show the vertically integrated moisture flux and its divergence for the winter (DJF) and summer (JJA), respectively, while Figures 5b and 5d show the E-P fields, respectively. Figures 5a and 5c show how the moisture is transported from the Atlantic Ocean to the Med region and Europe. The moisture flux is mostly eastward over the Med but with a southward component in the summer. The moisture flux over the Med Sea is somewhat stronger compared to the surrounding area due to additional local moisture available over the sea. The Med Sea is a moisture divergence zone both in winter and summer, indicating a local net moisture flux from the Sea to the surrounding atmospheric regions. The midlatitude to high-latitude continent area over the north of the Med and the tropical equator zone serve as the sink and source of moisture flux in winter, respectively. But, in summer, these two regions change their sink or source of moisture to the opposite as compared to the winter. This appropriately reflects the feature of seasonal adjustment of atmospheric general circulation over the study area. These results are quite consistent with *Mariotti et al.* [2002b]. However, the current divergence field results from the 20 km run depicts more detail, as for instance, the divergence field over the Fertile Crescent as well as the land-sea boundary areas can be more easily identified in the 20 km run. The E-P balances OF/A-IF/A very well as discussed before. However, as indicated in equation (3), the MFD should be also equal to E-P, and this can be verified by comparing Figures 5a and 5c to Figures 5b and 5d, i.e., E-P balances the MFD quite well. It is important to mention here that all the fields, which were used here for the calculation of the MBC, were taken from the 20 km run without any bias correction.

3.3. Analysis of the MBC Based on the Different Precipitation Categories

3.3.1. Over the Med

3.3.1.1. P and E

[20] All the main rainy months (October-March) during the research period were classified into five different groups

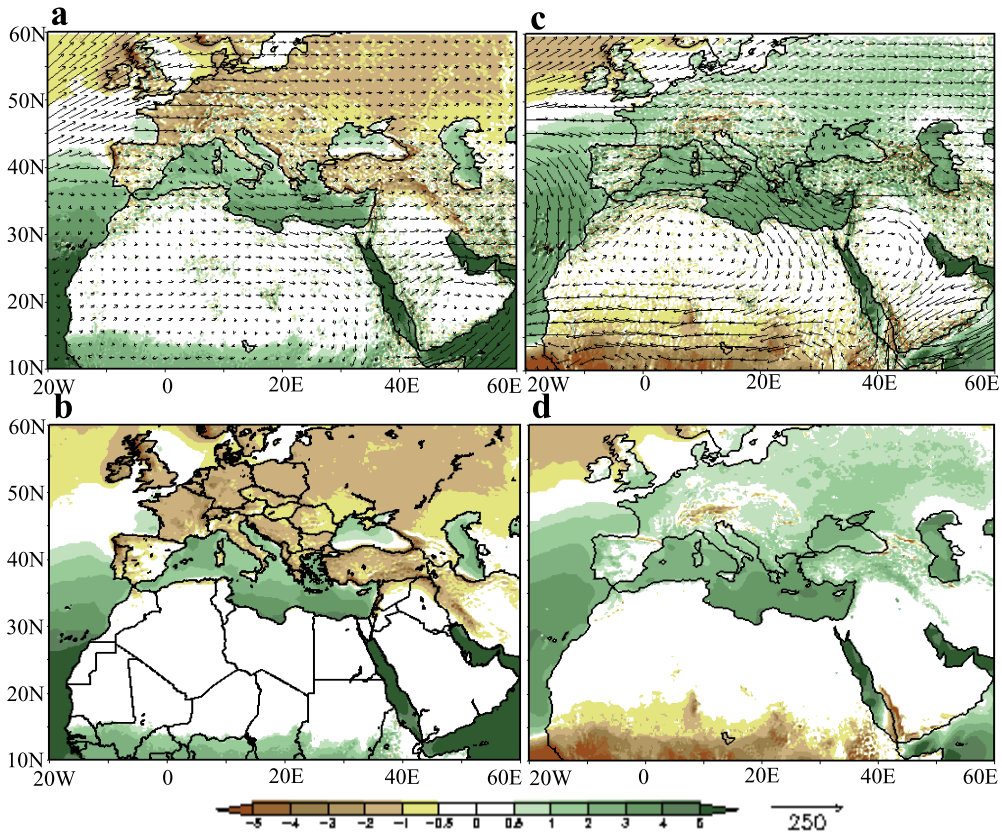

Figure 5. (a and b) Long-term (1979–2007) mean vertical integrated moisture flux (vectors, in kg/ms) and (c and d) moisture flux divergence (color, in mm/d) for the winter (DJF) (Figure 5a) and summer (JJA) (Figure 5c), and the evaporation minus precipitation (color, in mm/d) for the winter (Figure 5b) and summer (Figure 5d).

based on the amount of area mean monthly P. For convenience, the P categories were defined as follows: $P < 1.0$, $1.0 \le P < 1.5$, $1.5 \le P < 2.0$, $2.0 \le P < 2.5$, and $2.5 \le P$ (mm/d). For each P category, the means of the MBC and related parameters are calculated (Table 1 or Figure 6). The relationship between monthly P and other MBC will be discussed below.

[21] Table 1 and Figure 6 show that the mean precipitation of the rainy season is about 1.85 mm/d, while the mean E is about 2.44 mm/d. The area mean P is increasing

Table 1. Long-Term Seasonal Area Mean Moisture Budget Components Calculated Based on the Five Different Precipitation Categories[a]

		P < 1	1 < = p < 1.5	1.5 < = p < 2	2 < = p < 2.5	2.5 < = P	Mean or Sum
Month (percentage)		7 (4%)	41 (25%)	54 (32%)	46 (27%)	20 (12%)	168
West	inflow	0.90	0.97	1.17	1.41	1.27	1.19
	outflow	0.12	0.08	0.06	0.06	0.01	0.06
East	inflow	0.00	0.00	0.00	0.01	0.00	0.00
	outflow	0.84	1.05	1.22	1.25	1.52	1.21
North	inflow	0.92	0.60	0.56	0.42	0.67	0.56
	outflow	0.49	0.38	0.62	0.81	0.90	0.64
South	inflow	0.06	0.07	0.23	0.36	0.63	0.27
	outflow	1.35	0.95	0.71	0.58	0.43	0.73
Total inflow (TI)		1.88	1.65	1.96	2.20	2.58	2.02
Total outflow (TO)		2.80	2.47	2.61	2.70	2.87	2.64
TO-TI		0.92	0.82	0.65	0.50	0.29	0.62
Ave P		0.90	1.29	1.76	2.24	2.72	1.85
Ave E		1.99	2.19	2.38	2.60	2.85	2.44
E-P		1.09	0.90	0.63	0.37	0.14	0.58
Recycling ratio		51%	57%	55%	54%	53%	55%

[a]Long-term is 1979–2007 and seasonal is October through March. P is precipitation. West, east, north, and south stand for four different boundaries, and E is evaporation. The unit is mm/d, except for the recycling ratio and number of months, in which units are percentage and number of months.

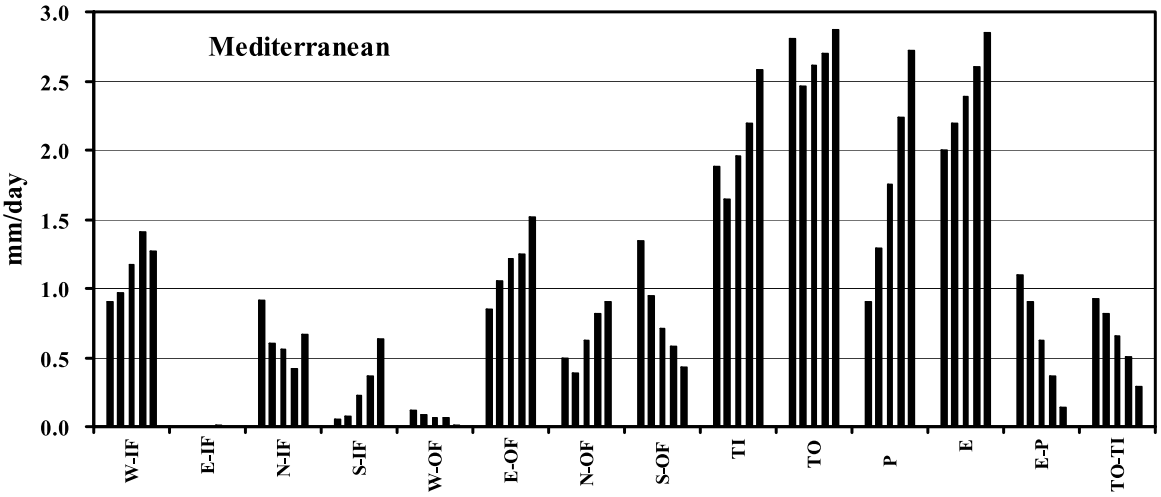

Figure 6. Long-term (1979–2007) seasonal (October to March) monthly mean of moisture budget components over the Mediterranean. The five columns in each group represent five increasing precipitation categories (left to right) from less than 1 to over 2.5 mm/d (details in the text). The different components along the *x* axis from left to right are as follows: W-IF,E-IF, N-IF, S-IF are the west, east, north, and south lateral boundary inflow (IF); next are the four corresponding outflow (OF) components; next are TI-total inflow, TO-total outflow, P-precipitation, E-evaporation, E-P, and TO-TI.

from 0.90 to 2.72 mm/d through the lowest to the highest precipitation category. The largest two precipitation categories contribute over 50% of the total seasonal rainfall. Comparing the P with *Mariotti et al.* [2002b] and *Jin and Zangvil* [2010], in which studies were carried out based mainly on the reanalysis data, we found that the P results from these three studies are quite close to each other. However, the 20 km's P is somewhat higher than theirs due to much higher spatial resolution data used here. The E value is lower than that of *Jin and Zangvil* [2010], and this can be explained by the different research area, i.e., both land and water here, while Jin and Zangvil covers mainly the water body.

[22] Figure 6 shows that the E is markedly increasing with the rising of the P category. E goes from 1.99 up to 2.85 mm/d from the lowest to the highest P category. A plausible explanation could be that the increase of P is usually associated with intensified cyclone activity and hence higher wind speeds which benefits the evaporation E. This point was illustrated as important for cumulus parameterization over the Med by *Stein and Alpert* [1991]. On the other hand, though E values change from the lowest to the highest P category is just less than 1 mm/d, the contribution of E to the P cannot be ignored. The Med Sea not only supports additional moisture to the cyclones which pass through this region during the winter, but also the relatively warmer sea surface has an important role. It enhances cyclones or accelerates the regenesis of cyclone through, for instance, the mechanism of convective instability of the second kind (CISK), especially over the eastern Med as suggested by *Alpert and Neeman* [1992]. It is interesting to note that the E reported by *Jin and Zangvil* [2010] is decreasing with the P for the first two categories, only then it starts to increase with the P, while here it increases for all categories. This is probably due to the different size of the research domain and the location between these two studies.

3.3.1.2. Boundaries Moisture Flux

[23] Table 1 and Figure 6 show that except for the first precipitation category, both the total inflow and the total outflow are increasing with the rising of the P category, from 1.65 to 2.58 mm/d and from 2.47 to 2.87 mm/d, respectively. The only decreasing of both total inflow and outflow from the first to the second P category (Figure 6) is quite interesting. A plausible explanation for this phenomenon could be that the smallest P is mostly not generated by the typical cyclone activities but largely by the local convective processes. In that case, E is dominated by high solar insolation forcing as the cloud cover of the sky is relatively low. Therefore there is still considerable moisture available over the study area; it leads to a strong moisture flux even for the smallest P category. Because of the main part of research area is covered by the water bodies, the local evaporated water vapor together with the moisture transported from outside the research region make the total outflow always larger than the total inflow for each specific P category (Figure 6). Also, the gradient of increasing total inflow (~0.31 mm/d) from second P category to the last P category is larger than that of total outflow (~0.13 mm/d), implying that external moisture has an important role in generating large amounts of precipitation (Figure 6).

[24] To describe the quantitative contribution of moisture flux to P, we looked at the vertically integrated moisture flux from each of the four lateral boundaries of study area. For the moisture inflow, Figure 6 shows that the moisture inflow is mainly from the west and north boundaries with the average value of 1.19 and 0.56 mm/d, responsible for 59% and 28% of the total moisture inflow, respectively. However, the changes of moisture inflow with the P categories are different for these two boundaries. The west inflow is increasing with the rising of P categories generally, while

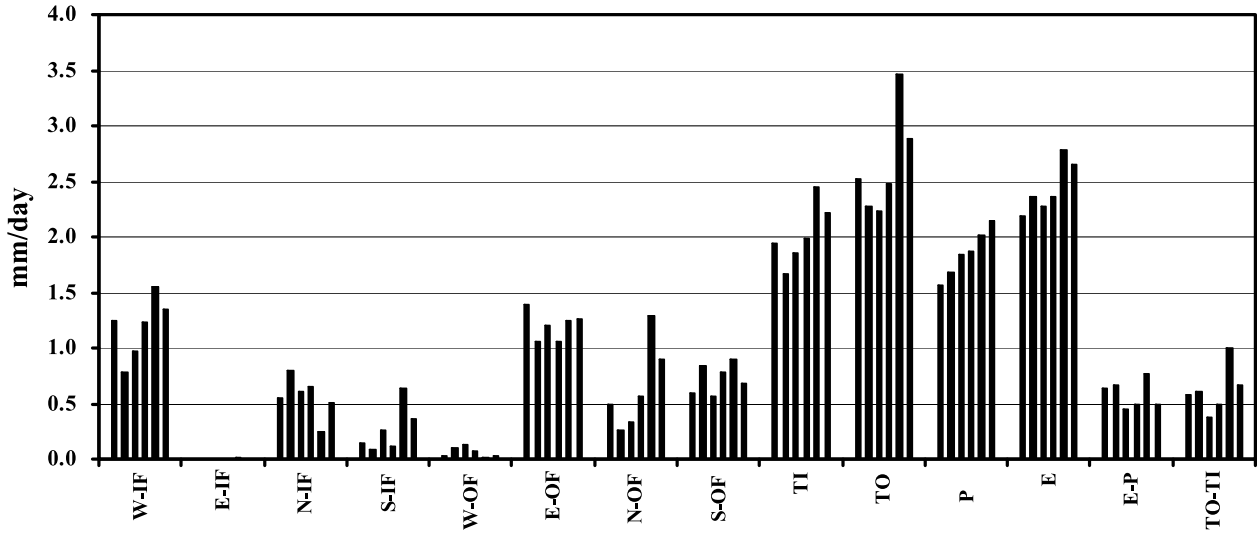

Figure 7. Long-term (1979–2007) seasonal (October to March) monthly mean moisture budget components sorted by the ascending of precipitation. For each group, the six columns present March, January, February, December, October, and November (from left to right). The different components along the *x* axis are as in Figure 6.

the north inflow is decreasing. This is because of the larger P is usually companied by a deeper upper air trough over the study area, and the enhanced northeastward air current by the deeper trough will depress the air current from the north. As expected, there is almost no moisture inflow from the east boundary as the research area is dominated by the westerly wind belt circulation. The finding of west inflow is the main source of moisture is consistent with *Jin and Zangvil* [2010]. Though the south boundary contributes little moisture to the research region, it increases significantly with the rising of the P categories; especially for the largest P category, the south boundary has almost the same value as the west boundary. This means that the moisture flux from the south boundary is not ignorable in the production of large amounts of precipitation. For the moisture outflow, Figure 6 shows that the moisture mainly flows out through the east, south, and north boundaries, with the value of 1.21, 0.73, and 0.64 mm/d, responsible for 46%, 27%, and 24% of the total moisture outflow. The change of outflow with the P category on the east, north, and south boundaries are exactly the reasonable responding to those changes on the boundary inflow restrained by the mass conservation law, i.e., an increasing trend on the east and north boundary, which decreasing trend in the south boundary. Again, the changes of E-P and OF/A-IF/A are consistent with each other quite well for all P categories, and E-P is larger than OF/A-IF/A for the first two smaller P categories, while E-P is less than OF/A-IF/A for the last two larger P categories (Figure 6).

3.3.1.3. Recycling Ratio

[25] For all the P categories, the R is larger than 50% with the average value of about 55% (Table 1). It means that the local evaporated moisture acts a critical role in the contribution of P over the research region. An important finding is that R is decreasing with the increasing of P category (Table 1). As discussed before, the E is increasing with P category. Therefore based on equation (5), it can be deduced that in order to get a decreasing of R, the increasing of total inflow should be much larger than that of increasing of E. It indirectly proves that the outside moisture also acts an essential role, epically in supporting relatively large P events. The value of R derived from this study is far larger than that of *Jin and Zangvil* [2010], in which they got only 18% over the eastern Med. That is because the current research area is about 20 times larger than theirs, and R is usually increasing with the increasing of the size of research domain, while the characteristic of surface cover is kept similar. Several studies have reported that the size of the research domain has a crucial influence to the moisture budget studies [i.e., *Berbery and Rasmusson*, 1999; *Shay-El et al.*, 1999]. A larger area better represents the reality of the large-scale moisture budget field, with the minimum area required about 1×10^5 km^2 [*Yeh et al.*, 1998]. Since our research area is much larger than that minimum required for moisture budget study, our results not limited by this factor.

3.3.1.4. Monthly Analysis of the MBC

[26] The mean MBC based on each individual month during the rainy season was also studied here. Figure 7 shows that, in general, the MBC for different month displays the same feature as shown in Figure 6. For example, for every month, the moisture inflow mostly comes from the west and the north boundaries, while the max moisture outflow is on the east boundary, etc. However, there are some very interesting results from this specific month-by-month analysis. The largest average basin precipitation values were found for October and November with the mean values of 2.01 and 2.15 mm/d, respectively. It is important to check whether these results represent the reality of the P regime over the research area. Actually, there are not sufficient P observations over the water bodies. Therefore only the observation data over the land area, which is within the

Table 2. Comparisons of Long-Term Seasonal Monthly Area Mean Moisture Budget Components for the East and West Mediterranean[a]

MBC		East Med	West Med
Inflow (IF)	west	7.71	5.55
	east	0.00	0.11
	north	0.39	2.54
	south	0.42	0.60
Outflow (OF)	west	0.00	0.19
	east	5.88	5.80
	north	2.44	1.29
	south	2.50	2.72
Total_IF (TI)		8.52	8.80
Total_OF (TO)		10.82	10.00
TO-TI		2.30	1.20
Precipitation (P)		2.14	2.29
Evaporation (E)		4.48	3.59
E-P		2.34	1.30
Recycling ratio		34%	29%

[a]Long-term is 1979–2007 and seasonal is October through March. Moisture budget component is MBC and Mediterranean is Med. Units are mm/d, except for the recycling ratio, in which the unit is percentage.

research domain, were used to test this feature, such as the countries over the Middle East, western and Eastern Europe, etc. Historical statistical data of P shows that, except to the Middle East countries, autumn indeed has the maximum monthly P over other parts of the land areas. For instance, in Spain, the maximum monthly P is on November for Madrid and on October for Barcelona and Valencia; in Italy, it is on November for Venice, Naples, Florence, Milan, and Rome. The similar findings were also confirmed by checking some of the eastern European countries within the research area, such as Bulgaria, Croatia, and Romania, etc. (The source for the cities' precipitation comes from the Web site of World Meteorological Organization.) *Jin and Zangvil* [2010] got the monthly maximum P in winter, since their research area was only over the eastern Med. Other interesting results derived from the monthly MBC analysis here (Figure 7) are that, for instance, the monthly minimum P is on March but with relative larger moisture inflow, while the month of October has the maximum moisture inflow and outflow as well as the highest E. These findings are in good agreement with *Jin and Zangvil* [2010]. They explained that the

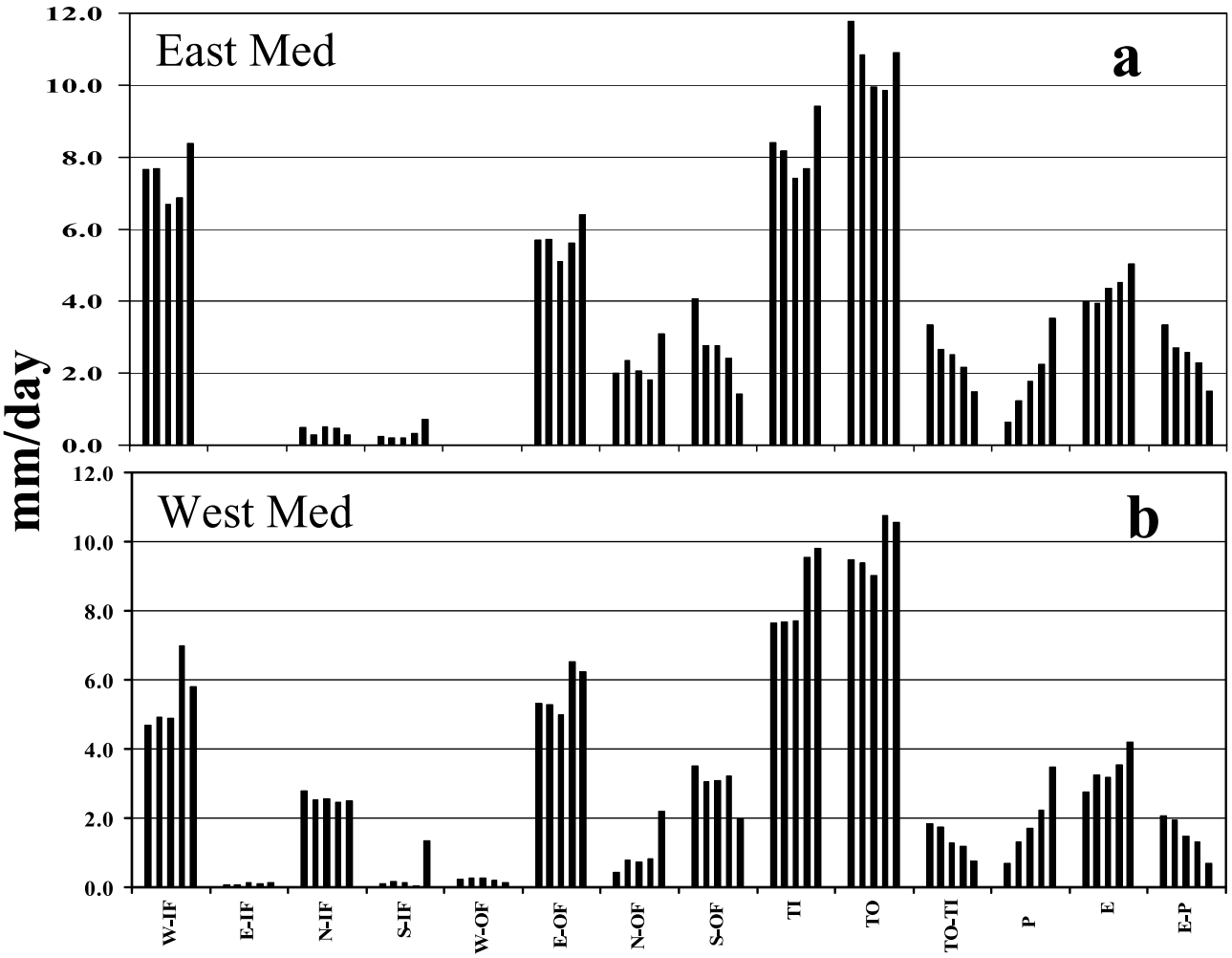

Figure 8. Same as Figure 6 but for the east and the west Mediterranean. The different components along the *x* axis are as in Figure 6.

Table 3. Table of Seasonal Mean Precipitation and Evaporation Based on the Five Precipitation Categories Both for Current and Future[a]

	Current				Future			
Precipitation Categories	Month	Percentage	Mean P	Mean E	Month	Percentage	Mean P	Mean E
P < 1	7	4%	0.9	1.99	19	13%	0.75	2.18
1.5 > p > = 1	41	24%	1.29	2.19	33	23%	1.26	2.36
2 > p > = 1.5	54	32%	1.76	2.38	61	42%	1.72	2.61
2.5 > p > = 2	46	27%	2.24	2.60	23	16%	2.17	2.82
P > = 2.5	20	12%	2.72	2.85	8	6%	2.75	3.20
Sum (or mean)	168	100%	1.85	2.44	144	100%	1.62	2.56

[a]Seasonal is October through March. P is precipitation and E is evaporation. Current is 1979–2007 and future is 2075–2099. Also included are columns for number of months and percentages for each category. The units of P and E are mm/d.

maximum moisture flux found in autumn is probably due to the fact that the sea surface temperature is still high and the air is relatively dry in autumn, a feature which accelerates the E process and makes more moisture available over the study area.

3.3.2. Over the Eastern and the Western Med

[27] The same analysis was also performed for two small selected rectangular basins over the eastern and western part of the Med separately, in order to be able to compare the MBC features for these two different areas. In general, the MBC changes with P category in the eastern and western Med shows the similar feature like that for the whole Med region though there are some important differences (Table 2 or Figure 8). Table 2 shows that the area average P for the eastern and the western Med are 2.14 and 2.29 mm/d and for E are 4.48 and 3.59 mm/d, respectively. The higher P in the western Med probably due to its geographical location in a strong cyclogenesis region (Genoa); also more abundant moisture is available as the west Med which is closer to the Atlantic Ocean. The higher E in the eastern Med region is due to its proximity to the arid Middle East region, and the relatively dry air surrounding it which clearly benefits E. The recycling ratios R are 34% and 29% for eastern and western Med, respectively. The significant decrease in R as compared to 55% over the entire Med is due to the much smaller domain. The larger R over east Med can be explained by the higher E as well as reduced total inflow over the EM (Table 2).

[28] Figures 8a and 8b show the MBC for the east and west Med based on the different P categories. There are some similar features for these two basins, as for example, the E is increasing with P, the west moisture inflow is the main contributor to the total inflow, E-P balances OF/A-IF/A quite well and the similar patterns of both total inflow and total outflow changing with P, etc. However, there are also remarkable differences between east and west epically on moisture fluxes from the boundaries. For instance, the contributions of mean west inflow to the total inflow are 90% and 63% for the east and the west Med, while for the north boundary they are 5% and 29%, respectively. The contributions of mean north outflow to the total outflow are 23% and 13% for the east and west Med, respectively (Table 2 or Figures 8a and 8b).

3.4. Changes of the MBC in the Future and Potential Mechanism for the Change

[29] The changes of MBC for the future (2075–2099) under the A1B emission scenario projected by the 20 km GCM were investigated here. The same P categories as the control run were also used for the future in order to be able to compare to the control run. Table 3 presents the mean P and E for different P categories both for the current and future runs. The area mean P is decreasing over the Med from 1.85 to 1.62 mm/d, while the Med mean E is increasing from 2.44 to 2.56 mm/d between the current and the future. It should be highlighted here that *Jin et al.* [2010] found different E anomalies for land (decreasing) and sea (increasing) bodies separately over the study area. The only increasing E anomaly found here is because we consider the research area as whole. The precipitation event for the smallest P category, i.e., P < 1 mm/d, is significantly increasing from 4% to 13%, while the largest P category, i.e., P ≥ 2.5 mm/d, is dramatically decreasing from 12% to only 6% between the current and future run. However, the most frequent precipitation event remains in the middle P (1.5 ≤ P < 2 mm/d) category both for the current and control run, but the percentage of this category out of the total events is increasing from 32% to 42% between current and future. Another interesting finding is that the value of mean P for most of P categories show decreasing trends between current and future; only for the largest P category, the mean value of P is slightly increasing, from 2.72 to 2.75 mm/d (Table 3 or Figure 9). This change predicted by the 20 km model is consistent with observed increases in extreme rainfall. For example, *Alpert et al.* [2002] found a decreasing trend of P together with an increasing mean value of the extreme P events based on rain gauge observations. (Notice that *Alpert et al.* [2002] analysis was based on daily rainfall for 1950–1995, while here similar trends are shown for the future based on mean monthly rainfall data.) The increasing E between current and future is probably due to the higher sea surface temperature and the air temperature, projected in the A1B emission scenario.

[30] The change in the boundary moisture fluxes between future and current climate is shown in Figure 9. For the inflow, a general increasing trend can be seen both on the west and north boundaries. The higher inflow from the west boundary could result from the enhanced E over the Atlantic Ocean, which is then transported to the Med. The more moisture inflow from the north boundary is perhaps due to the 20 km model prediction of a wetter rain season for the middle to high-latitude region in the future [*Mariotti et al.*, 2008; *Jin et al.*, 2011]; therefore the more moisture evaporates and transfers to the Med also from the north boundary. On the other hand, the model predicts a drier rain season over the subtropics which leads to a decrease in the moisture inflow from the south boundary (Figure 9). For the outflow,

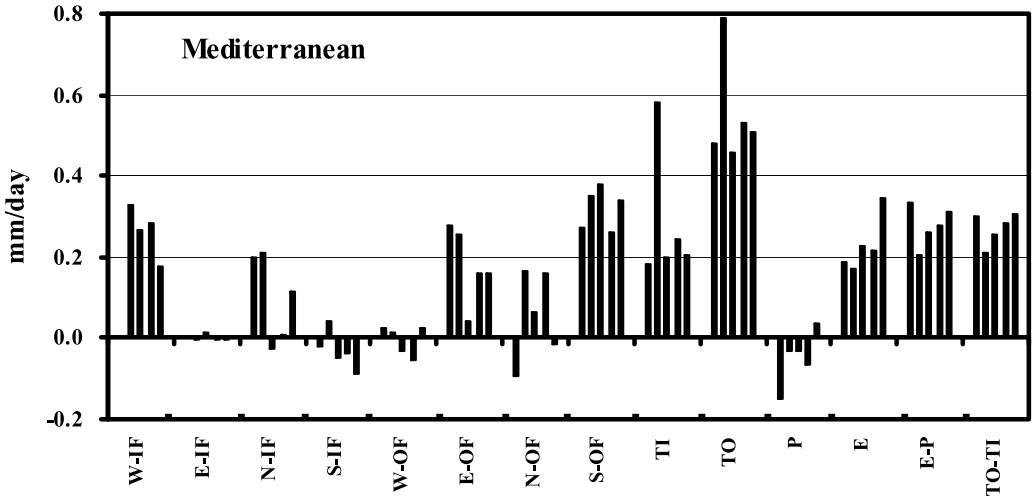

Figure 9. Same as Figure 6 but for the changes of the moisture budget components between future (2075–2099) and current (1979–2007) 20 km GCM run (future minus current). Positive values indicate increases by the end of the 21st century. The different components along the *x* axis are as in Figure 6.

because of the increasing of inflow and E over the Med as discussed above, these result in a higher moisture outflow on the east, south, and north boundaries in the future. All the changes of boundary moisture fluxes result in both increasing of total inflow and total outflow for the specific P categories in the future (Figure 9).

[31] The potential mechanisms that control the change of MBC results in the 20 km GCM data has been discussed by *Jin et al.* [2011]. The change of moisture transport pattern is the main reason which influences the future change of MBC over the study area. The large-scale drying mechanism was related to some adjustment of the atmospheric general circulation, such as the poleward expansion of the Hadley Cell as proposed by *Lu et al.* [2007]. The descending air of Hadley Cell suppresses precipitation by drying the lower troposphere and therefore expands the subtropical dry zones. At the same time, and related to this, the rain-bearing midlatitude storm tracks also shift poleward.

4. Conclusions

[32] The relationships between the precipitation and other moisture budget components over the Mediterranean were carried out by using JMA 20 km super-high-resolution GCM data. We found that generally, over the Mediterranean, the outflow-inflow is balancing the independently calculated E-P quite well with the correlation coefficient of 0.89, and the mean error between these two terms is only 0.15 mm/d. Separate analyses for the eastern and western Med show that the correlation coefficient between these two terms is quite high reaching 0.98 and 0.94, respectively. These results lend high credibility to the moisture budget calculations based on the 20 km climate model data.

[33] The seasonal (October-March) P of current run over the Mediterranean simulated from the 20 km GCM showed a quite reasonable agreement with the CRU. Especially, the 20 km showed its credible performance in capturing the peak P which is highly influenced by the complex physiographical effects typical for the Med region. The vertically integrated moisture flux and its divergence both for the winter (DJF) and the summer (JJA) of current run simulated by the 20 km GCM show much sharper patterns in comparison with earlier studies based on the reanalysis data and coarse resolution climate models.

[34] The study of the moisture budget components for the present climate show that the seasonal area mean precipitation and evaporation are 1.85 mm/d and 2.44 mm/d, respectively. These values are higher than that of *Mariotti et al.* [2002b] and *Jin and Zangvil* [2010]. The largest two precipitation categories contribute over 50% of the total seasonal rainfall. The evaporation increases with the increasing of the precipitation category, as well as the relatively high mean recycling ratio (55%) indicate that the local evaporation has an important role in influencing the local precipitation. In addition, the decreasing trend of the recycling ratio, R, with the rising of precipitation category also implies that the outside moisture inflow has an essential role in generating large amount of precipitation. Both the total inflow and total outflow are increasing with the rising precipitation category. For each precipitation category, the total outflow is larger than the total inflow shows that the research area is a main source of moisture since the research area is largely covered by seawater. Individual boundary moisture fluxes show that the main moisture is from the west boundary and contributes 59% of the total inflow, while the main outflow is through the east boundary and is responsible for 46% of total outflow. Analysis of monthly precipitation indicates that the October and November have the two largest amounts of precipitation over the Med region, and the historical observation data confirms this finding. This fact further proves the credibility of the 20 km GCM data.

[35] The separated moisture budget components study for the east and the west Mediterranean show that the area mean precipitation for the east and the west Mediterranean are 2.14 and 2.29 mm/d, while the evaporation are 4.48 and 3.59 mm/d. The plausible reason for the differences has been discussed. The moisture supplies to the east Mediter-

ranean is mainly from the west boundary, while for the west Mediterranean, the north boundary inflow also has an important role except for the west boundary. The future moisture budget components over the study area show that the precipitation is decreasing from 1.85 to 1.62 mm/d, and the evaporation is increasing from 2.44 to 2.56 mm/d between current and future. The most important finding is that the largest precipitation event out of the total precipitation events is decreasing from 12% to only 6%. However, the intensity of this heavy precipitation category is enhanced in the future. This interesting change is only found for the largest precipitation events.

[36] Overall, the 20 km GCM showed credible performance in the simulation of the moisture budget components changing with the precipitation over the Med. This research shows that the climate model can be a very useful tool to study the moisture budget, especially for the future climate change which is impossible to perform with the reanalysis data.

References

Adler, R. F., et al. (2003), The Version−2 Global Precipitation Climatology Project (GPCP) monthly precipitation analysis (1979−Present), *J. Hydrometeorol.*, *4*, 1147–1167, doi:10.1175/1525-7541(2003)004<1147:TVGPCP>2.0.CO;2.

Alpert, P., and B. U. Neeman (1992), Cold small-scale cyclones over the eastern Mediterranean, *Tellus, Ser. A*, *44*, 173–179.

Alpert, P., and Y. Shay-El (1994), The moisture source for the winter cyclones in the Eastern Mediterranean, *Isr. Meteorol. Res. Pap*, *5*, 20–27.

Alpert, P., et al. (2002), The paradoxical increase of Mediterranean extreme daily rainfall in spite of decrease in total values, *Geophys. Res. Lett.*, *29*(11), 1536, doi:10.1029/2001GL013554.

Alpert, P., I. Osetinsky, B. Ziv, and H. Shafir (2004), Semi-objective classification for daily synoptic systems: Application to the Eastern Mediterranean climate change, *Int. J. Climatol.*, *24*, 1001–1011, doi:10.1002/joc.1036.

Alpert, P., C. Price, S. O. Krichak, B. Ziv, H. Saaroni, I. Osetinsky, J. Barkan, and P. Kishcha (2005), Tropical tele-connections to the Mediterranean climate and weather, *Adv. Geosci.*, *2*, 157–160, doi:10.5194/adgeo-2-157-2005.

Alpert, P., S. O. Krichak, I. Osetinsky, M. Dayan, D. Haim, and H. Shafir (2008), Climatic trends to extremes employing regional modeling and statistical interpretation over the E. Mediterranean, *Global Planet. Change*, *63*, 163–170, doi:10.1016/j.gloplacha.2008.03.003.

Berbery, E. H., and E. M. Rasmusson (1999), Mississippi moisture budgets on regional scale, *Mon. Weather Rev.*, *127*, 2654–2673, doi:10.1175/1520-0493(1999)127<2654:MMBORS>2.0.CO;2.

Diaz, H. F., M. P. Holerling, and J. K. Eischeid (2001), ENSO variability, teleconnections and climate change, *Int. J. Climatol.*, *21*, 1845–1862, doi:10.1002/joc.631.

Fraedrich, K. (1994), ENSO impact on Europe?—A review, *Tellus, Ser. A*, *46*, 541–552.

Fraedrich, K., and K. Mueller (1992), Climate anomalies in Europe associated with ENSO extremes, *Int. J. Climatol.*, *12*, 25–31, doi:10.1002/joc.3370120104.

Gibelin, A. L., and M. Deque (2003), Anthropogenic climate change over the Mediterranean region simulated by a global variable resolution model, *Clim. Dyn.*, *20*, 327–339.

Giorgi, F., and P. Lionello (2008), Climate change projections for the Mediterranean region, *Global Planet. Change*, *63*, 90–104, doi:10.1016/j.gloplacha.2007.09.005.

Hurrell, J. W., and H. van Loon (1997), Decadal variations in climate associated with then North Atlantic oscillation, *Clim. Change*, *36*, 301–326, doi:10.1023/A:1005314315270.

Intergovernmental Panel on Climate Change (2007), *Fourth Assessment Report: Working Group II Report "Impacts, Adaptation and Vulnerability*," Cambridge Univ. Press, Cambridge, U. K.

Jin, F. J., and A. Zangvil (2010), Relationship between moisture budget components over the eastern Mediterranean, *Int. J. Climatol.*, *30*(5), 733–742, doi:10.1002/joc.1911.

Jin, F. J., A. Kitoh, and P. Alpert (2010), Global warming projected water cycle changes over the Mediterranean, East and West: A comparison study of a super-high resolution global model with CMIP3, *Philos. Trans. A*, *368*, 5137–5149, doi:10.1098/rsta.2010.0204.

Jin, F. J., A. Kitoh, and P. Alpert (2011), The atmospheric moisture budget over the Eastern Mediterranean based on a high-resolution global model—Past and future, *Int. J. Climatol.*, in press.

Krichak, S. O., P. Alpert, and M. Dayan (2004), The role of atmospheric processes associated with hurricane plga in the December 2001 floods in Israel, *J. Hydrometeorol.*, *5*(6), 1259–1270, doi:10.1175/JHM-399.1.

Lu, J., G. Vecchi, and T. Reichler (2007), Expansion of the Hadley cell under global warming, *Geophys. Res. Lett.*, *34*, L06805, doi:10.1029/2006GL028443.

Mariotti, A., N. Zeng, and K.-M. Lau (2002a), Euro-Mediterranean rainfall and ENSO - a seasonally varying relationship, *Geophys. Res. Lett.*, *29*(12), 1621, doi:10.1029/2001GL014248.

Mariotti, A., M. V. Struglia, N. Zeng, and K. M. Lau (2002b), The hydrological cycle in the Mediterranean region and implications for the water budget of the Mediterranean Sea, *J. Clim.*, *15*, 1674–1690, doi:10.1175/1520-0442(2002)015<1674:THCITM>2.0.CO;2.

Mariotti, A., N. Zeng, J. H. Yoon, V. Artale, A. Navarra, P. Alpert, and Z. X. Li (2008), Mediterranean water cycle changes: Transition to drier 21st century conditions in observations and CMIP3 simulations, *Environ. Res. Lett.*, *3*, 044001, doi:10.1088/1748-9326/3/4/044001.

Mitchell, T., and D. Jones (2005), An improved method of constructing a database of monthly climate observations and associated high-resolution grids, *Int. J. Climatol.*, *25*, 693–712, doi:10.1002/joc.1181.

Mizuta, R., K. Oouchi, H. Yoshimura, A. Noda, K. Katayama, S. Yukimoto, M. Hosaka, S. Kusunoki, H. Kawai, and M. Nakagawa (2006), 20-km-mesh global climate simulations using JMA-GSM model Mean climate states, *J. Meteorol. Soc. Jpn.*, *84*, 165–185, doi:10.2151/jmsj.84.165.

Mizuta, R., Y. Adachi, S. Yukimoto, and S. Kusunoki (2008), Estimation of the future distribution of sea surface temperature and sea ice using the CMIP3 multi-model ensemble mean, *Tech. Rep. 56*, 28 pp., Meteorol. Res. Inst., Ibaraki, Japan.

Ozsoy, E. (1981), On the atmospheric factors affecting the Levantine Sea, Tech. Rep. 25, 29 pp., Eur. Cent. for Medium Range Weather Forecasts, Reading, U. K.

Peixoto, J. P. (1973), Atmospheric vapor flux computations for hydrological purposes, *Publ. 357*, 83 pp., World Meteorol. Org., Geneva, Switzerland.

Price, C., L. Stone, A. Huppert, B. Rajagopalan, and P. Alpert (1998), A possible link between El Niño and precipitation in Israel, *Geophys. Res. Lett.*, *25*, 3963–3966, doi:10.1029/1998GL900098.

Rasmusson, E. M. (1967), Atmospheric water vapor transport and the water balance of North America. Part I: Characteristics of the water vapor flux field, *Mon. Weather Rev.*, *95*, 403–426, doi:10.1175/1520-0493(1967)095<0403:AWVTAT>2.3.CO;2.

Rasmusson, E. M. (1968), Atmospheric water vapor transport and the water balance of North America. Part II: Large-scale water balance investigations, *Mon. Weather Rev.*, *96*, 720–734, doi:10.1175/1520-0493(1968)096<0720:AWVTAT>2.0.CO;2.

Rasmusson, E. M. (1971), A study of the hydrology of eastern North America using atmospheric vapor flux data, *Mon. Weather Rev.*, *99*, 119–135, doi:10.1175/1520-0493(1971)099<0119:ASOTHO>2.3.CO;2.

Reddaway, J. M., and G. R. Bigg (1996), Climate change over the Mediterranean and links to the more general atmospheric circulation, *Int. J. Climatol.*, *16*, 651–661, doi:10.1002/(SICI)1097-0088(199606)16:6<651::AID-JOC27>3.0.CO;2-Z.

Rodwell, M. J., and B. J. Hoskins (1996), Monsoons and the dynamic of deserts, *Q. J. R. Meteorol. Soc.*, *122*, 1385–1404, doi:10.1002/qj.49712253408.

Shay-El, Y., P. Alpert, and A. Da Silva (1999), Reassessment of the moisture source over the Sahara Desert based on NASA reanalysis, *J. Geophys. Res.*, *104*, 2015–2030, doi:10.1029/1998JD200003.

Shay-El, Y., P. Alpert, and A. daSilva (2000), Preliminary estimation of horizontal fluxes of cloud liquid water in relation to subtropical moisture budget studies employing ISCCP, SSMI and GEOS-1/DAS datasets, *J. Geophys. Res.*, *105*, 18,067–18,089, doi:10.1029/1999JD901200.

Starr, V. P., and J. P. Peixoto (1958), On the global balance of water vapor and the hydrology of deserts, *Tellus*, *10*, 188–194, doi:10.1111/j.2153-3490.1958.tb02004.x.

Starr, V. P., J. P. Peixoto, and A. R. Crisi (1965), Hemispheric water balance for the IGF, *Tellus*, *17*, 463–472, doi:10.1111/j.2153-3490.1965.tb00209.x.

Stein, U., and P. Alpert (1991), Inclusion of sea moisture flux in the Anthes-Kuo cumulus parametrization, *Contrib. Atmos. Phys.*, *64*, 231–243.

Xie, P., and P. A. Arkin (1997), Global precipitation: A 17-year monthly analysis based on gauge observations, satellite estimates, and numerical model outputs, *Bull. Am. Meteorol. Soc.*, *78*, 2539–2558, doi:10.1175/1520-0477(1997)078<2539:GPAYMA>2.0.CO;2.

Yanai, M., S. Esbensen, and J. H. Chu (1973), Determination of average bulk properties of tropical cloud clusters from large-scale heat and moisture budgets, *J. Atmos. Sci.*, *30*, 611–627, doi:10.1175/1520-0469(1973)030<0611:DOBPOT>2.0.CO;2.

Yeh, P. J.-F., M. Irizarry, and E. A. B. Eltahir (1998), Hydroclimatology of Illinois: A comparison of monthly evaporation estimates based on atmospheric water balance and soil water balance, *J. Geophys. Res.*, *103*, 19,823–19,837, doi:10.1029/98JD01721.

Zangvil, A., D. H. Portis, and P. J. Lamb (1992), Interannual variations of the moisture budget over the Midwestern United States in relation to summer precipitation. Part II: Impact of local evaporation on precipitation, paper presented at Yale Mintz Memorial Symposium on Climate and Climate Change, Isr. Meteorol. Soc., Jerusalem.

Zangvil, A., D. H. Portis, and P. J. Lamb (2001), Investigation of the large-scale atmospheric moisture field over the Midwestern United States in relation to summer precipitation. Part I: Relationships between moisture budget components on different timescales, *J. Clim.*, *14*, 582–597, doi:10.1175/1520-0442(2001)014<0582:IOTLSA>2.0.CO;2.

Zangvil, A., D. H. Portis, and P. J. Lamb (2004), Investigation of the large-scale moisture field over the Midwestern United States in relation to summer precipitation. Part 2: Recycling of local evapotranspiration and association with soil moisture and crop yields, *J. Clim.*, *17*, 3283–3301, doi:10.1175/1520-0442(2004)017<3283:IOTLAM>2.0.CO;2.

Ziv, B., H. Saaroni, and P. Alpert (2004), The factors governing the summer regime of the Eastern Mediterranean, *Int. J. Climatol.*, *24*, 1859–1871, doi:10.1002/joc.1113.

Ziv, B., H. Saaroni, A. Baharad, D. Yekutieli, and P. Alpert (2005), Indications for aggravation in Summer heat conditions over the Mediterranean basin, *Geophys. Res. Lett.*, *32*, L12706, doi:10.1029/2005GL022796.

P. Alpert and F. Jin, Department of Geophysics and Planetary Sciences, Tel-Aviv University, Tel-Aviv 69978, Israel. (pinhas@post.tau.ac.il)

A. Kitoh, Meteorological Research Institute, Tsukuba, 305-0052, Japan.